RESEARCH ARTICLE

Dynamic optimization reveals alveolar epithelial cells as key mediators of host defense in invasive aspergillosis

Jan Ewald[1,2☯]*, Flora Rivieccio[3,4☯], Lukáš Radosa[3], Stefan Schuster[1]*, Axel A. Brakhage[3,4‡]*, Christoph Kaleta[5‡]

1 Department of Bioinformatics, Friedrich Schiller University Jena, Jena, Germany, 2 Center for Scalable Data Analytics and Artificial Intelligence (ScaDS.AI), University of Leipzig, Leipzig, Germany, 3 Department of Molecular and Applied Microbiology, Leibniz Institute for Natural Product Research and Infection Biology - Hans Knöll Institute (HKI), Jena, Germany, 4 Department of Microbiology and Molecular Biology, Institute of Microbiology, Friedrich Schiller University Jena, Jena, Germany, 5 Research Group Medical Systems Biology, Institute of Experimental Medicine, Kiel University, Kiel, Germany

☯ These authors contributed equally to this work.
‡ AAB and CK also contributed equally to this work.
* jan.ewald@uni-leipzig.de (JE); stefan.schu@uni-jena.de (SS); axel.brakhage@leibniz-hki.de (AAB)

Abstract

Aspergillus fumigatus is an important human fungal pathogen and its conidia are constantly inhaled by humans. In immunocompromised individuals, conidia can grow out as hyphae that damage lung epithelium. The resulting invasive aspergillosis is associated with devastating mortality rates. Since infection is a race between the innate immune system and the outgrowth of *A. fumigatus* conidia, we use dynamic optimization to obtain insight into the recruitment and depletion of alveolar macrophages and neutrophils. Using this model, we obtain key insights into major determinants of infection outcome on host and pathogen side. On the pathogen side, we predict *in silico* and confirm *in vitro* that germination speed is an important virulence trait of fungal pathogens due to the vulnerability of conidia against host defense. On the host side, we found that epithelial cells, which have been underappreciated, play a role in fungal clearance and are potent mediators of cytokine release. Both predictions were confirmed by *in vitro* experiments on established cell lines as well as primary lung cells. Further, our model affirms the importance of neutrophils in invasive aspergillosis and underlines that the role of macrophages remains elusive. We expect that our model will contribute to improvement of treatment protocols by focusing on the critical components of immune response to fungi but also fungal virulence traits.

Author summary

Fungal infections are an increasing problem and threat for individuals which suffer from an impairment of immune functions due to immunosuppressive therapies or diseases. In those patients the innate immune response is not able to efficiently clear fungal cells from body surfaces and stop an invasive growth into tissues and bloodstream infections.

Aspergillus fumigatus is a ubiquitous mold as well as potent pathogen causing life-threatening infections, invasive aspergillosis, via lung inhalation of fungal spores (conidia). The innate immune response against conidia in the lung alveoli is a highly dynamic process and involves the interplay of immune cells like macrophages and neutrophils as well as lung epithelial cells. In the presented study, we used the mathematical approach of dynamic optimization to understand the roles of human cells and virulence factors of *A. fumigatus* in a quantitative and time-resolved manner. Our model predicts that lung epithelial cells play an important role in fungal clearance and contribute to pro-inflammatory signaling by cytokine release upon conidial stimulation. Further, this so far underappreciated role of epithelial cells and other findings are supported by experiments with established cell lines and primary lung cells of mice as model host organism.

Introduction

Since we constantly inhale microorganisms, the human lung is an entry point for opportunistic pathogens, like the mold *Aspergillus fumigatus* [1, 2]. Besides being a saphrophyte involved in the decay of organic matter in soil, *A. fumigatus* possesses virulence characteristics such as small spores (conidia), a fast growth at body temperature and the production of specific proteins, carbohydrates and secondary metabolites allowing its immune evasion [3–7]. These traits enable *A. fumigatus* to reach the lung's alveoli and cause invasive aspergillosis by filamentous growth (hyphae) into the tissue and dissemination into the host [5, 8]. In immunocompetent hosts this is prevented by the fast and efficient clearance of conidia by the innate immune system within a few hours [7, 9]. However, once *A. fumigatus* grows invasively facilitated by a suppressed immune system, mortality is very high (30–95%) due to non-efficient diagnostics and limited treatment options [10–13].

Along with the advances in medical care the number of patients with defects and suppression of their immune system is expected to grow. Major causes for this trend are the increasing number of cancer patients receiving chemotherapy [14, 15], organ transplant recipients [16] or patients with acquired immune deficiency syndrome (AIDS) [17]. Most recently, a high number of COVID-19 patients in intensive care units with extensive ventilation has been accompanied with secondary fungal infections due to *Aspergillus spp*. [13, 18].

The race between fungal growth and host immune response is complex and involves many cells like alveolar epithelial cells (AEC), alveolar macrophages (AM) and recruited neutrophils [7, 9]. To better understand this spatial and dynamic process computational modeling has proven to be of value [19–24]. These models are based on agent-based modelling or differential equation systems and contribute to a better understanding of the immune response. In particular, the meaning of spatial-dynamics of AM clearing conidia [20, 22, 23, 25] as well as the influence of the initial fungal burden on clearance and persistence of *A. fumigatus* were studied [19]. A major achievement and advantage of *in silico* models is the integration of existing biological knowledge and the generation of new hypotheses by disclosing knowledge gaps.

Despite extensive modeling and experimental investigations, the relative contribution of individual host immune cell types in invasive aspergillosis remains elusive [8]. For example, AM were identified as phagocytes of conidia [26] and release cytokines upon fungal infection [27]. Yet, AM depletion in mice at early phases of infection showed no effect on mortality while depletion of neutrophils was accompanied with low survival rates [28]. Current models and their analysis are based on immune cells and virtually neglect the contribution of AEC to cytokine release and fungal clearance. Experimental data obtained *in vitro*, however, suggest

that AEC can act as potent phagocytes [29] and release a significant amount of cytokines during their interaction with conidia [30]. Additionally, the importance of AEC in the promotion of neutrophil recruitment has been shown *in vivo* [31] and it has been postulated that AEC represent a 'neglected portal entry of *Aspergillus*' [7]. Therefore, the focus of our presented model here, is to dissect the contributions of AEC and innate immune cells for defense against *A. fumigatus*.

To elucidate the dynamic process of invasive aspergillosis during the first 24h, we propose a model using dynamic optimization as a mathematical approach. The mathematical concept of a dynamic system described by differential equations and regulated by control variables matches the dynamics of the innate immune response with recruitment and depletion of neutrophils and AM (mainly by maturation of monocytes). Due to this advantage, dynamic optimization has also been used to model other host-pathogen interactions and immune responses [24, 32–34] and makes use of the fact that these energy-demanding processes are highly optimized during evolution [35]. Our presented model, in addition, not only elucidates the complex recruitment dynamics of immune cells, but we also studied the role of AEC during early stages of fungal infection. To proof key variables of the model and thus its validity, major findings like fungal germination and cytokine release were experimentally evaluated.

Results

Model overview

The aim and scope of our modeling are a better understanding of the decisive parameters and interactions contributing to infection by *A. fumigatus* in the first 24h. To this end, we model the different growth states of *A. fumigatus* and their interaction with the innate immune response in the lung alveoli during the first hours of infection (see Fig 1). In addition, we explicitly model AEC as interactive cells and consider a single dose scenario of fungal conidia exposure. The latter modeling decision enables comparison of results and parameters to experimental animal models, which mainly use single dose regimes [36, 37].

Our model based on ordinary differential equations (ODE) considers time-dependent transition kinetics to describe the process of swelling and germination of conidia (detailed description in Subsection Model formulation). After germination, growth of *A. fumigatus* as hyphae depends on the presence of AEC as resource. Importantly, we accurately model interaction of each cell type with all host cell types. Resting conidia are far less recognized or killed due to their coating and swollen conidia are phagocytosed and killed by AM, neutrophils and AEC. Since AM and AEC are unable to phagocytose and kill larger hyphae at reasonable rates [38, 39], we only model killing of hyphae by neutrophils.

Host cell dynamics are characterized by damage, host or pathogen mediated, and transmigration of immune cells. In our dynamic optimization model, AEC face lysis by hyphae and damage by activated immune cells. While AM and neutrophils like AEC show cell death upon interaction with fungal cells, their transmigration upon infection is modeled by recruitment and depletion. In fact, the changes in cell number in our model can reflect also cell proliferation or programmed cell death. However, for simplicity we refer in the following to it as transmigration by recruitment and depletion including all other processes of host cell number control.

The maximal rate of recruitment and depletion is linked to the presence of pro-inflammatory cytokines and is optimized in our dynamic optimization approach via the control variables u_{1-4} (see Fig 1 and *cf*. Materials and methods, Subsection Model formulation). In our model we capture the release of cytokines by AM as well as AEC to reveal their respective contribution during infection.
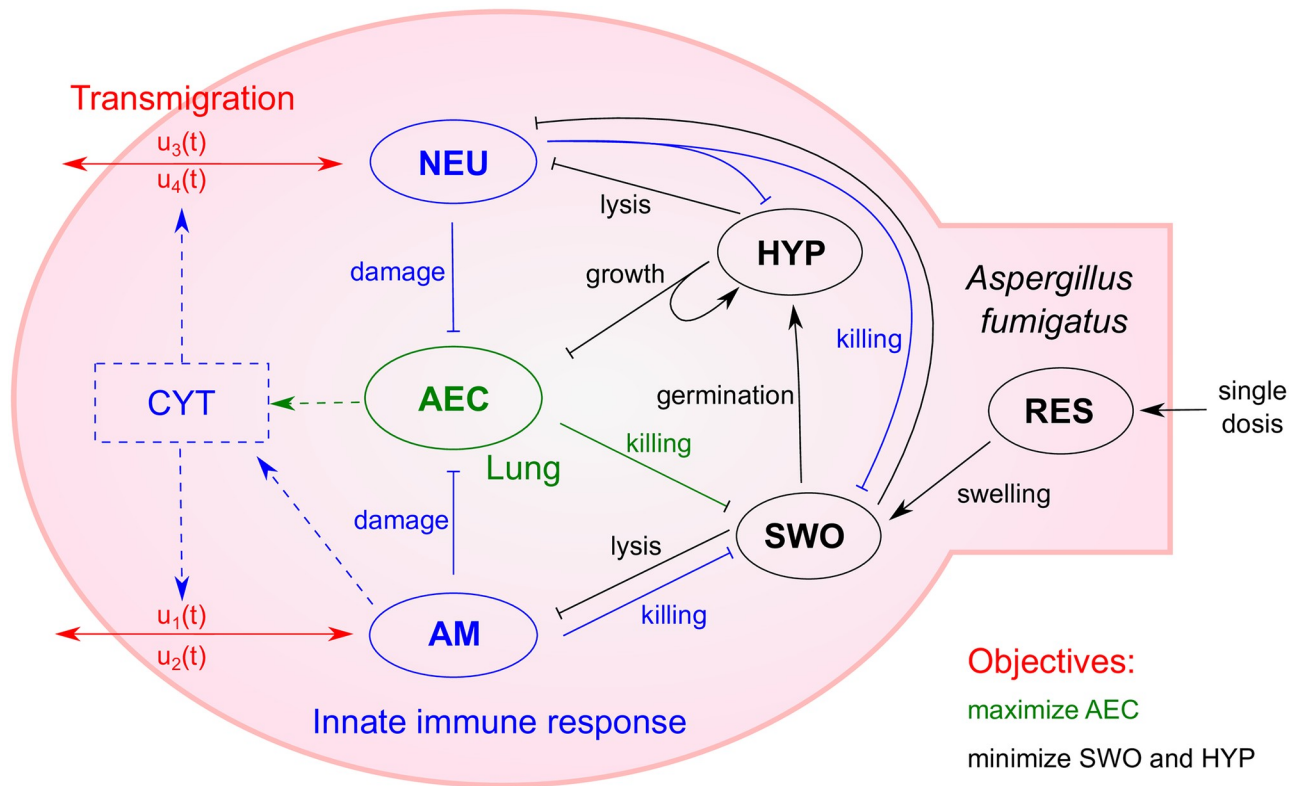
Fig 1. Model of invasive aspergillosis and the innate immune response as dynamic optimization problem. The different fungal growth states (black) including resting conidia (RES), swollen conidia (SWO) and hyphae (HYP) interact with alveolar epithelial cells (AEC, green) as well as with neutrophils (NEU, blue) or alveolar macrophages (AM, blue). Immune cell population is optimized via transmigration (red), which is linked to the cytokine level (CYT, blue), and optimal recruitment and depletion attain the trade-off between pathogen minimization and tissue integrity. Arrow heads indicate a positive interaction and bars show negative interactions.

https://doi.org/10.1371/journal.pcbi.1009645.g001

As host objectives we define two main goals, which are optimized during infection. Firstly, active fungal cells (swollen conidia and hyphae) should be minimized at all time points to avoid systemic infection. Secondly, unnecessary tissue damage *e.g.* due to hyperinflammation and collateral damage mediated by immune cells must be minimized. The consideration of only one of the objectives leads to undesired dynamics like continued hyphal growth or extensive tissue damage, as shown in S2 Appendix. Hence, we performed optimization with an equal weighting of both objectives. We did not opt for an alternative formulation of the objective function like the inclusion of energy requirements of the immune response or a more detailed quantification of the weighting between those objectives. This is mainly due to the difficulty of quantification of the related parameters (energy requirements) and the lack of time course data required for a multi-objective dynamic optimization (inverse optimal control) [40].

Parameters and time course of early immune response

For our dynamic optimization model of the innate immune response during early invasive aspergillosis, reference parameters were estimated based on an extensive study of existing data and literature (see S1 Appendix). The model focuses on the events in the alveoli during the first 24h and we normalize all cell populations per alveolus. Experimental studies and data reveal that the average number of AEC is 11.4 (type I and II combined) in a healthy mouse [41, 42]. Type I cells cover up to 95% of the alveolar surface and are more likely to come in contact

with conidia, while type II cells are more responsible for tissue repair and integrity [43]. Further, both types of cells can secrete pro-inflammatory cytokines upon stimulation [44]. Hence, we combined both cell types for the sake of simplicity as AEC in our model. On average in every third or fourth alveolus an AM, respectively a neutrophil, is resident [45]. In animal models of invasive aspergillosis typically initial conidia doses of 10^5 to 10^7 are applied as single dose [7, 37]. Since there are around $2.3 \cdot 10^6$ alveoli in a murine lung [42] and not all conidia reach an alveolus, one resting conidium per alveolus relates to a typical fungal burden during experiments.

To elucidate the general pattern of innate immune response during invasive aspergillosis, we simulated 500 randomized parameter sets, where each parameter follows a log-normal distribution with the estimated reference value as the mode (maximum of distribution). The calculated time courses of the dynamic optimization reveal that healthy mice are able to clear even high fungal burden without a complete destruction of the epithelial cell barrier (see Fig 2 and details of solving the dynamic optimization in Subsection Solving the optimization problem and parameter sensitivity). This is achieved by a rapid cytokine release by AM as well as AEC and recruitment of neutrophils after conidial swelling. After 10 to 15h, recruitment of neutrophils is stopped and the immune cells are depleted to avoid unnecessary tissue damage. In this regard, our model well reflects experimental observations [46] and depicts the trade-off between pathogen clearance and tissue damage by the innate immune response. In our model, interestingly, AM are not recruited in large quantities and are mostly depleted after germination of conidia. Based on our estimated parameters of the kinetic rates, this is mostly due to slower killing of conidia compared to neutrophils and the ability of AEC to release cytokines in large quantities.

Parameter sensitivity reveals importance of fungal growth parameters

To better understand the roles of immune cells and AEC, we analyzed parameter sensitivity and simulated several scenarios to study the effect of immunodeficiencies and dosage of conidia.

We determined decisive parameters for the outcome of infection by calculating the contribution to variance in the objective function of each randomized parameter (see Materials and methods, Subsection Solving the optimization problem and parameter sensitivity). Further, we simulated healthy mice and lack of immune cells as well as the influence of low or high doses of conidia. Across all scenarios the fungal parameters s_1 (germination time of a swollen conidium) and h_1 (hyphal growth rate) are most decisive for infection outcome since they explain more than 50% of the variance in the objective function (see Fig 3). This illustrates that fast germination of swollen conidia is a strong virulence attribute, because it is the most vulnerable growth state of the pathogen. The growth rate of hyphae is in addition crucial in the race between neutrophils (recruitment and hyphal killing) and *A. fumigatus*.

On the host side, the importance of some parameters differs significantly when the initial fungal burden is altered. Interestingly, at lower doses immune cell parameters like the number of resident neutrophils $N(0)$ or rate of hyphal killing h_2 are important (see Fig 3). However, at higher doses parameters of AEC, such as conidia phagocytosis (s_4) or cytokine release (c_2), are more important for the infection outcome and contribute nearly 20% to the variance in the objective function. The parameter sensitivity and time course of infection indicate that at low doses the control of hyphal growth is most important, while at high doses AEC are crucial to lower the number of swollen conidia. These results are noteworthy since parameters related to functions of AM only show even when combined a minor influence on the infection outcome (3.7% at high dose and 9.5% at low dose). Typically, AM are extensively studied since they
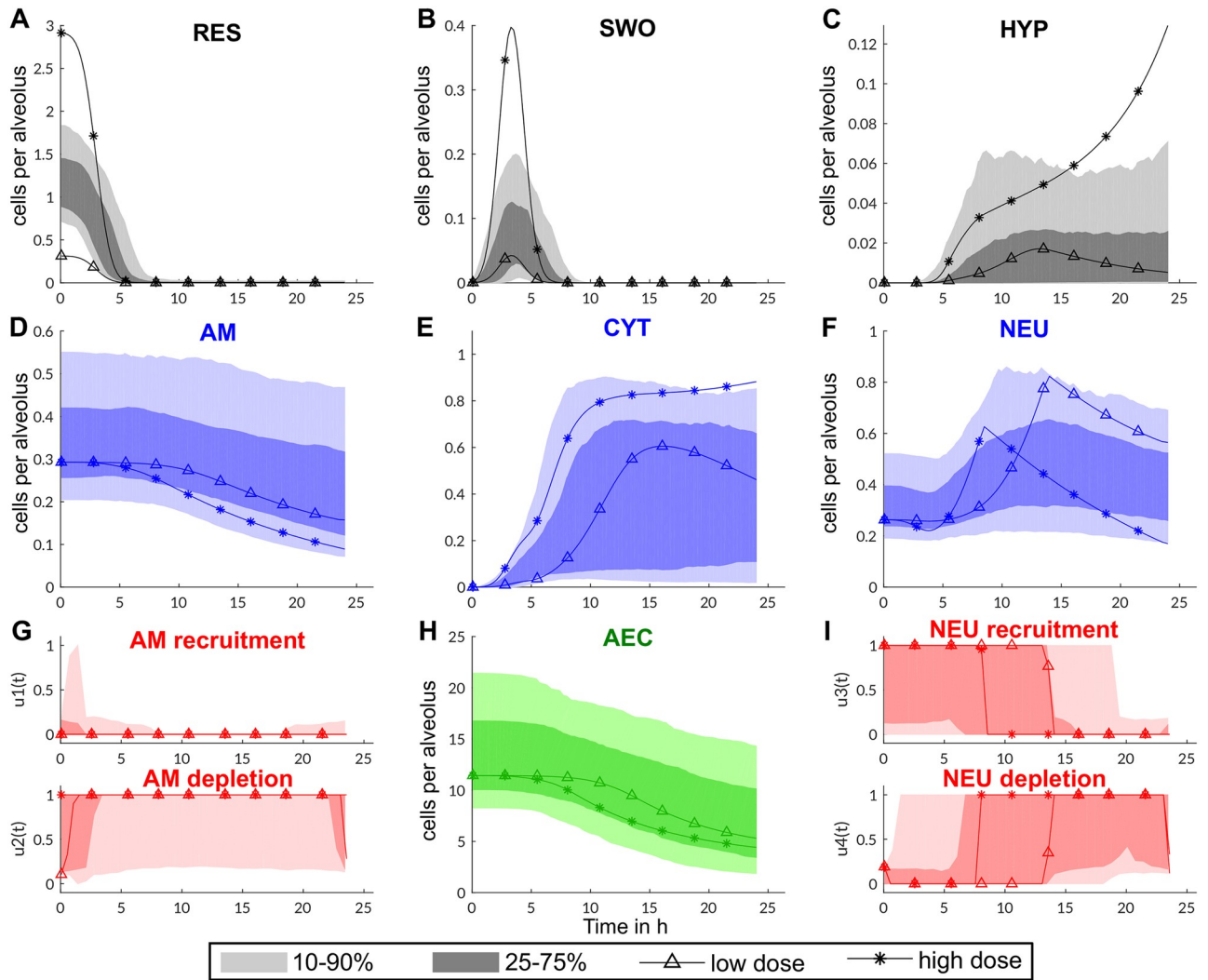
Fig 2. Dynamics of innate immune response of the murine host for varying parameters (shadings) and two dose scenarios of conidia based on the reference parameter set (lines). A-C Dynamics of fungal cells per alveolus. **D, F** show the dynamics of the immune cells per alveolus which are influenced by the optimized recruitment and depletion rates in panels **G** and **I** (rates between 1, maximal, and 0, no recruitment/depletion). Recruitment and depletion potential is dependent on the cytokine level (**E**). Cytokines are produced by alveolar macrophages (**D**) and alveolar epithelial cells (**H**) in response to swollen conidia (**B**) or hyphae (**C**). The simulations of 500 parameter sets are depicted with shadings indicating the confidence intervals of time courses.

belong to the first line of defense. However, our parameter sensitivity results do not disclose a singular and distinctive role and we therefore performed additional analyses in the following sections.

Further insights were gained by studying the changes in parameter influence under scenarios of immunodeficiencies like the lack of monocytes (progenitor cells of AM) or neutrophils which were simulated as reduced immune cell populations and recruitment rates (1% of normal value). In both scenarios simulating monocytopenia or neutropenia, fungal virulence factors are even more important for infection outcome (see Fig 3). But there are different tendencies as to which factor is more important. During monocytopenia, here for simplicity expressed as a lack of AM, the time span for germination, s_1, is more important. This suggests that AM are mainly involved in the control of swollen conidia (see Fig 3). In contrast, during
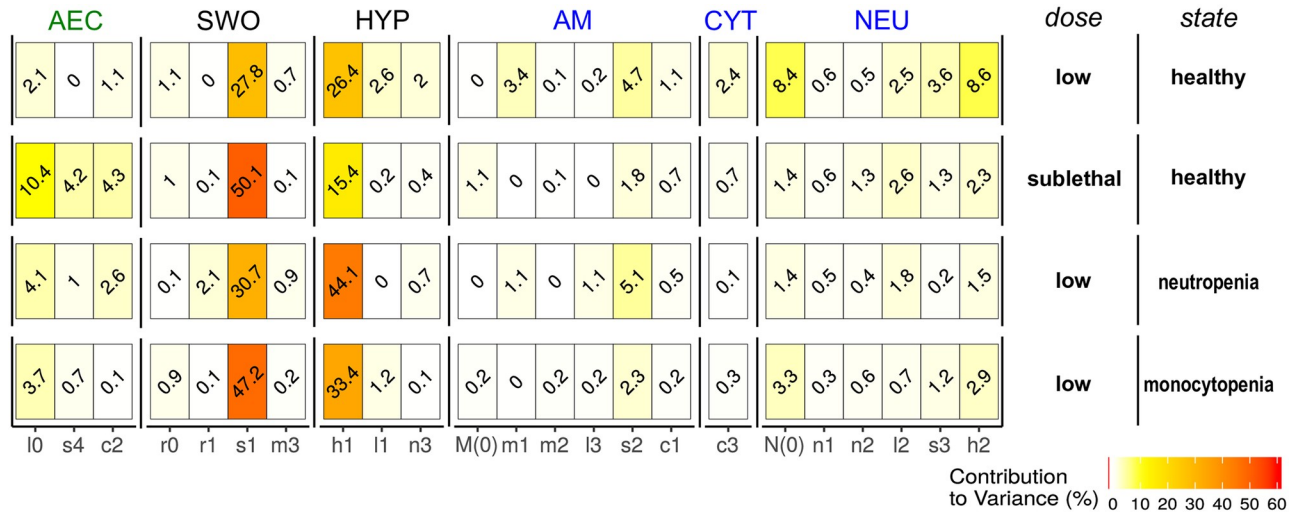
Fig 3. Influence of parameters on the outcome of infection depicted by the contribution to variance (colored from white, yellow to red from no to high influence). This relative contribution is based on a Spearman rank correlation of the parameter value and the objective value of the optimal solution (see Materials and methods, Subsection Solving the optimization problem and parameter sensitivity). Parameters are grouped based on their relation to cell types: alveolar epithelial cells (AEC), resting (RES) or swollen conidia (SWO), hyphae (HYP), alveolar macrophages (AM) and neutrophils (NEU). In addition the cytokine (CYT) property c_3 (decay rate) is listed.

neutropenia the hyphal growth rate is more decisive for the infection outcome (see Fig 3) supporting the observation that neutrophils are crucial to prevent filamentous growth.

To support the findings established by modeling, we performed an experimental investigation of fungal virulence parameters by the comparison of different *Aspergillus* species. As revealed by the parameter sensitivity analysis, a key virulence factor is fast germination to minimize the time period of the vulnerable swollen-conidia state. The common species *A. fumigatus*, *A. nidulans*, *A. niger* and *A. terreus* show differences in their germination kinetics at 37°C, where *A. nidulans* is fastest, *A. fumigatus* as well as *A. niger* are around 1–2h slower and *A. terreus* is by far the slowest with an average germination time of > 24h (see Fig 4A and 4B). Our model predicts here a non-linear but distinctive relationship between the germination time and epithelial damage after 24h (see Fig 4C). It suggests that virulence expressed as epithelial damage is strongly reduced if the germination time is longer than 10h.

Strikingly, in an experimental set-up where human (A549 cell line) and murine (T7 cell line) lung AEC are co-incubated with *Aspergillus spp.* for 24h, only those species with fast germination showed a pronounced host cell damage (see Fig 4D and 4E and *cf*. S1 Fig for different multiplicities of infection). Moreover, cytotoxicity against human cells coincides with germination speed and strongly supports model prediction. However, we observed a higher cytotoxicity of *A. fumigatus* against murine AEC while other species show comparable results (see Fig 4E). This underlines the importance of further investigations to understand differences between the human host and rodent model organisms. Further, it suggests an avoidance of elevated epithelial damage by *A. fumigatus* and its ability to hide and escape in AEC during the human immune response.

The accordance of prediction based on modeling with experimental data on germination as well as cytotoxicity shows that our dynamic optimization approach is able to identify key parameters of invasive aspergillosis. However, since *A. fumigatus* is the most common cause of invasive aspergillosis [10] in spite of its slightly slower germination than *A. nidulans*, the interaction of fungal pathogens with host cells and parameters defining this process require additional decisive factors for infection outcome.
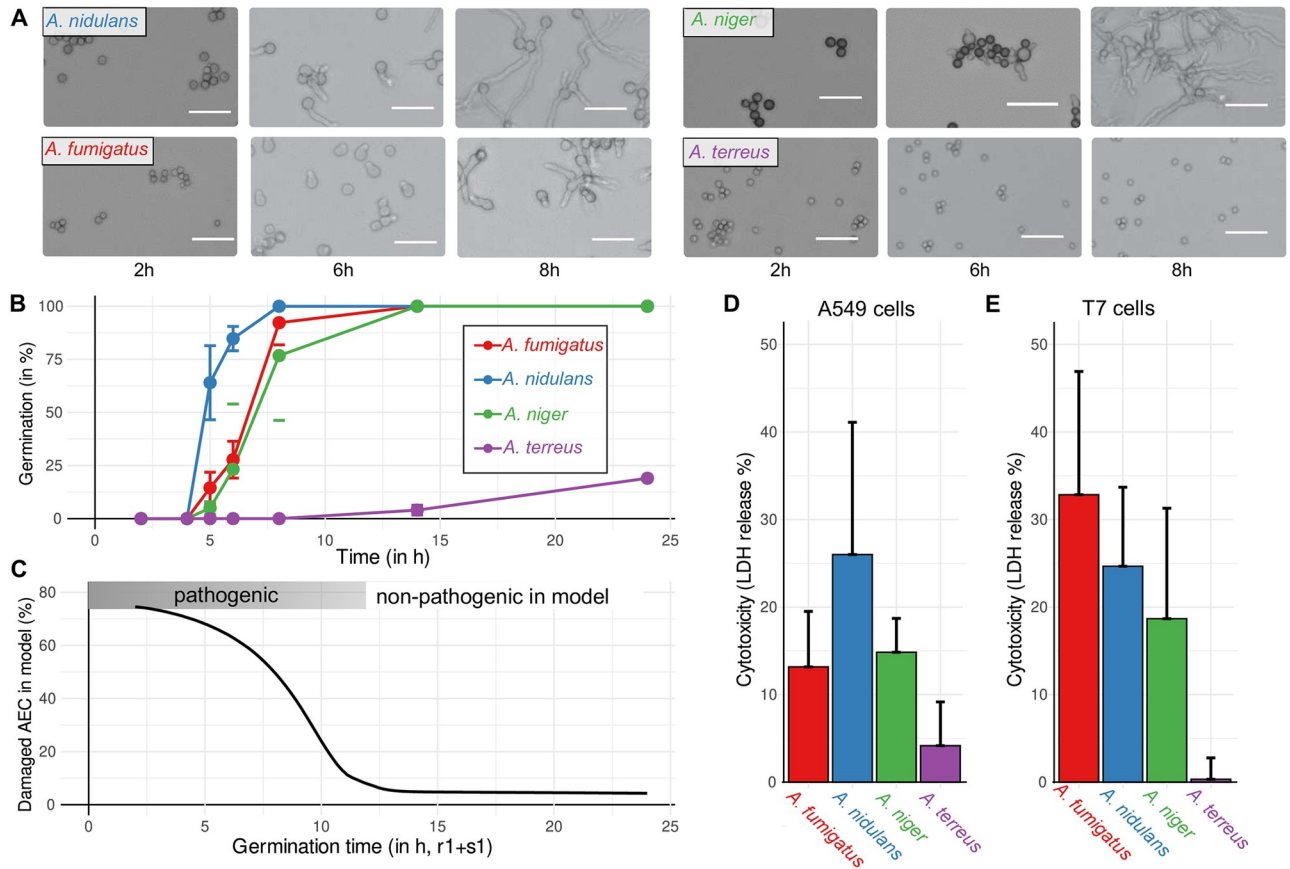
Fig 4. Germination kinetics of *Aspergillus spp*. and its impact on epithelial cytotoxicity. A Microscopic images (white scale bar, 20μm) of germination assays on RPMI medium to automatically count and derive germination kinetics as shown in **B** for the species *A. fumigatus* (red), *A. nidulans* (blue), *A. niger* (green) and *A. terreus* (purple). Error bars represent the standard deviation of four replicates. **C** the relation of germination time and damage of AEC after 24h in the dynamic optimization model and parameter range with expected pathogenicity. Model prediction in **C** is compared to experimental cytotoxicity of *Aspergillus spp*. by lactate-dehydrogenase (LDH) release measurements after 24h co-incubation with human A549 epithelial cells in **D** and with murine T7 epithelial cells in **E**. Error bars represent the standard deviation of six replicates.

To this end, in the following part the specific roles and functions of host cells are investigated by modeling and supported by experimental investigations.

Neutrophils and epithelial cells primarily promote fungal clearance and cytokine release

The advantage of our model is that we can suppress a host cell population or function *in silico* to study their role and importance for infection outcome. This way we can simulate animal models with immunodeficiencies like neutropenia that is triggered by usage of cyclophosphamide and cortisone acetate in murine models of invasive aspergillosis [47]. The analysis of parameter sensitivity provides a global overview about the correlation between infection parameters and infection outcome. However, the causality of parameter influence is not explained. To this end, we performed additional *in silico* experiments with varying conidial doses to understand and link host cell functions to infection outcome.

The conidia dose-response-curves clearly indicate that lack of neutrophils heavily worsens infection outcome across all dose scenarios and host damage is barely dose-dependent (see Fig 5A and 5B). Further, both objectives, *i.e.*, the preservation of tissue and reduction of the fungal
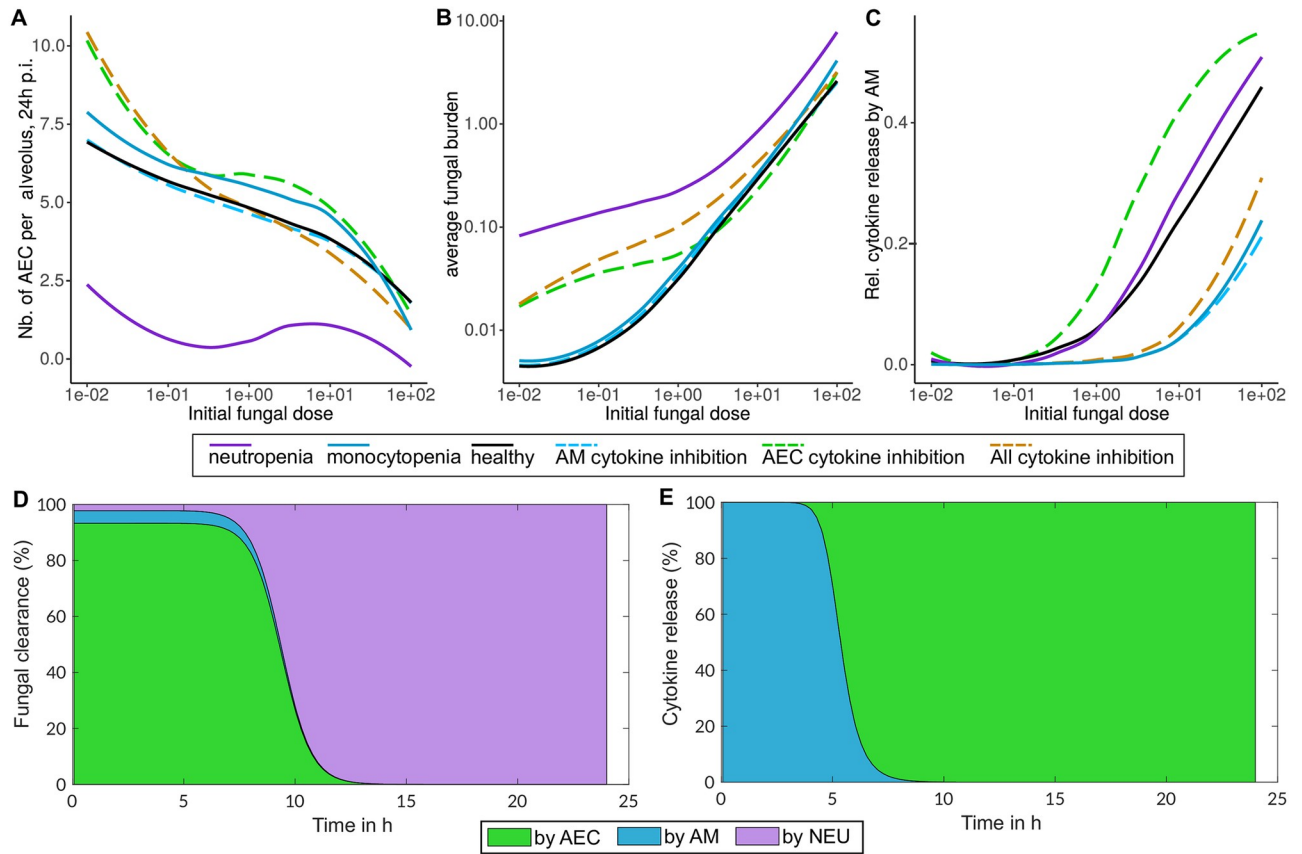
Fig 5. Relative contribution of host cells during infection. A-C Dose-response-curves with varying conidia doses (x-axis) and the remaining number of epithelial cells at the end of simulation in **A** or the average fungal burden during simulation in **B**. The relative contribution of alveolar macrophages to cytokine release depending on the initial conidia dose in **C**. Response curves were determined for the following disturbances: lack of immune cells (1% neutrophils, solid violet; 1% macrophages solid light blue) and cytokine release inhibition (1% of cytokine release by alveolar macrophages (AM, dashed light blue), 1% release by alveolar epithelial cells (AEC, dashed green) or 1% release from both (dashed brown). **D, E** Role of macrophages (AM), neutrophils (NEU) and epithelial cells (AEC) in fungal clearance **D** and cytokine release **E** in the dynamic optimization model over time as percentage of total at each time point. Fungal clearance is calculated as the sum of killing all fungal cell types (conidia and hyphae).

https://doi.org/10.1371/journal.pcbi.1009645.g005

burden, are more impaired by neutropenia than by all other deficiency scenarios including lack of AM or an inhibition of cytokine release. Interestingly, lack of AM or an inhibition of cytokine release by AM show no major differences in the infection outcome compared to the reference parameter set of healthy mice (see Fig 5A and 5B). The optimization results for the inhibition of cytokine release by AEC or by both, AEC and AM, indicate a shift in the immune objective at low conidia dosage. In comparison to healthy mice, lung tissue is more preserved at low conidia concentrations, but with the drawback of a higher average of fungal burden during the simulated time of infection.

In our model AM and AEC exhibit overlapping functions and duties during infection. Both are able to clear swollen conidia and to release cytokines for immune cell recruitment. However, their contribution is different depending on the initial fungal burden and during the dynamic stages of infection. When the dose of conidia is low, the relative contribution of AM to cytokine production is nearly zero and most importantly, germination and hyphal growth are recognized by AEC (see Fig 5C). The relative contribution to cytokine release by AM rises to > 40% at very high conidia concentrations (see Fig 5C) indicating that AM are more important when a high number of swollen conidia is present (10–100 spores per alveolus).

This finding is supported by the relative contribution of each cell type to fungal clearance and cytokine release over the time course of infection (see Fig 5D). During infection, according to our model, AM are responsible for early recognition of conidia, whereas AEC are the main cytokine releasing cells after germination. However, the low quantity of AM compared to AEC, lead to a much higher cytokine release by AEC compared to AM in absolute and relative terms during infection (see Fig 5E).

The prominent role of AEC in pro-inflammatory cytokine production and their major contribution to phagocytosis is not captured by other models of invasive aspergillosis [19, 21] and indicates an underestimated importance of these cells for the immune response. To quantify and support findings predicted by our model, *ex vivo* experiments with murine cells were performed and pro-inflammatory cytokines (TNF)-α and (IL)-6 were measured upon stimulation with *A. fumigatus* by enzyme-linked immunosorbent assay (ELISA). These cytokines were selected because of their prominent role during invasive aspergillosis in mice [46, 48–50]. Whereas AM mainly produce (TNF)-α after 6h of infection with conidia, murine AEC mainly produce (IL)-6 after 10h (see Fig 6A). At similar cell counts AM produce earlier (6h versus 10h), but less in absolute terms in comparison to AEC when excess release upon conidial challenge of both cytokines, (TNF)-α and (IL)-6, is combined (see Fig 6B). Considering the higher number of AEC than AM in an alveolus, these experimental findings strongly support our model that AEC are important mediators of the immune response.

Moreover, our model reveals that AEC are important phagocytes and are predicted to be the main cell type clearing fungal spores in the first hours of infection (see Fig 5D). Nevertheless, after germination neutrophils are decisive for fungal clearance by killing hyphae. These findings highlight that the alveolar epithelial cells fulfill a major role in fungal clearance but also in immune cell recruitment by cytokine release.

Discussion

In this study we deduced a unique model based on dynamic optimization to better understand the innate immune response during invasive aspergillosis. Main and distinctive features of the model are the optimization of the recruitment of immune cells depicting the trade-off between tissue integrity and pathogen clearance (dynamic optimization) as well as the active role of lung AEC in the immune response. While there is uncertainty in the kinetic description of the infection dynamics, it clearly provides a time-resolved insight into the roles of host cells and factors contributing to virulence. Further, the possibility to consider several cell types and inclusion of non-metabolic processes is a big advantage over other modeling techniques like flux balance analysis or statistical thermodynamics [51, 52].

The simulations and analyses of our model revealed key parameters and distinctive roles of host cells during the innate immune response against *A. fumigatus* and other Aspergilli. We identified the morphotype 'swollen conidia' to be most vulnerable for the attack by the host. Hence, the duration of this state is minimized by the fungus in order to escape phagocytosis and, subsequently, outcompete host cells by fast growth of hyphae. While this was indicated by experimental studies linking fungal traits with clinical observations [53, 54], we here report a quantification of this relationship. Further, we provide experimental evidence by determining the germination kinetics of different *Aspergillus spp.*. Further evidence for our model is given by data on the cytotoxicity against human and murine AEC by these fungi. Our results support the finding that the highly virulent strain of *A. fumigatus* CEA10 possesses a faster and higher germination rate in the lung environment accompanied with a more extensive lung damage than the less virulent strain Af293 [55]. Interestingly, in our and other studies *A. nidulans* showed fastest germination and a rather high damage to AEC. Since *A. nidulans* is not the
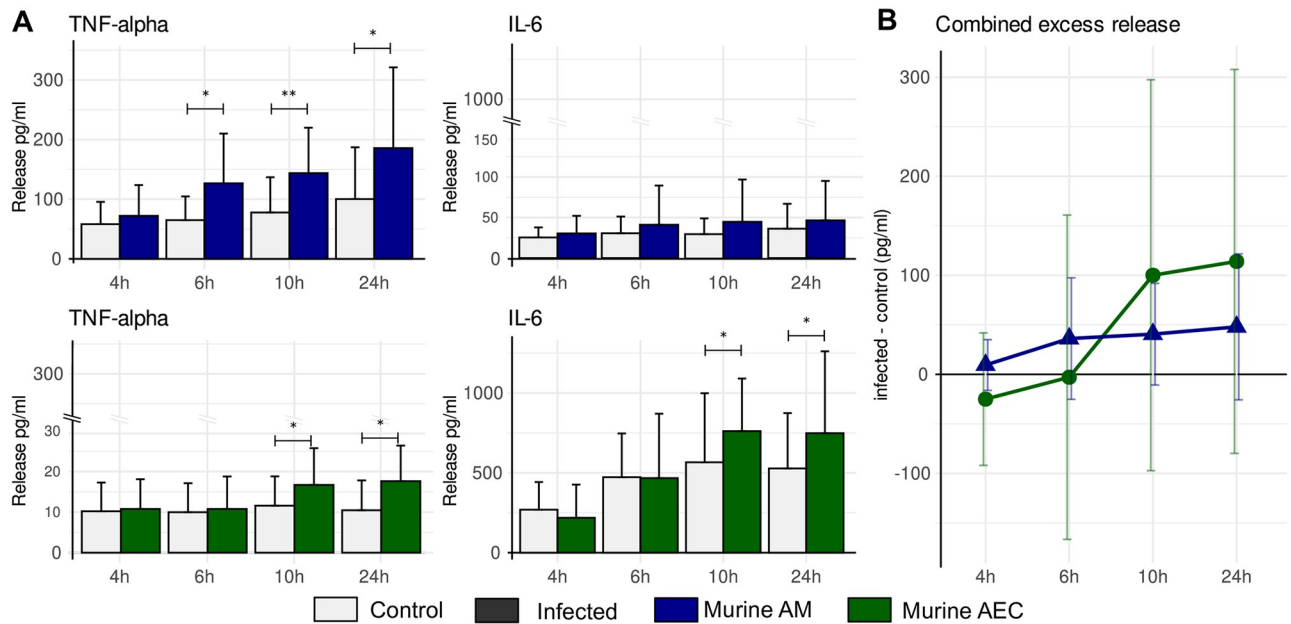
Fig 6. *Ex vivo* **cytokine release of isolated murine alveolar macrophages (AM, blue) and epithelial cells (AEC, green) upon infection with *A. fumigatus*. A** Release of (TNF)-α and (IL)-6 over time in infected and control cells measured by ELISA. Significant differences between control and infected cells were determined by a two-tailed and paired t-test indicated by * ($p < 0.05$) and ** ($p < 0.01$). Error bars represent the standard deviation from nine mice used for cell isolation. **B** Combined cytokine release of both (TNF)-α and (IL)-6 in excess over spontaneous release over time to depict contribution during early and later stages of fungal infection.

leading cause of invasive aspergillosis in humans [56], it is likely that this species lacks immune evasion mechanisms in comparison to *A. fumigatus* [38]. Hence, important fungal virulence traits of *A. fumigatus* are presumably linked to an efficient escape or inhibition of phagocytosis in comparison to *A. nidulans*. This conclusion is supported by the observation that *A. fumigatus* showed stronger cytotoxicity against murine cells in comparison to human AEC (see Fig 4D and 4E). While this indicates an adaption of *A. fumigatus* to hide and reside in human AEC from other immune cells, further investigation is necessary to understand the differences between the human host and rodent model organisms.

As crucial host parameters for infection outcome we reaffirmed the importance of neutrophils to control filamentous growth of *A. fumigatus* which confirms that dysfunctional hyphal killing by lack of neutrophils or non-functional neutrophils is a major risk factor for invasive aspergillosis [28, 57]. In addition to immune effector cells, we found that lung AEC significantly contribute to the immune response by phagocytosis of conidia and cytokine release in response to fungal germination. While this finding was partially observed and suggested in previous studies, we here present the first model which quantifies the role of AEC. Together with experimental measurements that compare the cytokine release of AM and AEC, we conclude that the role of AEC is underestimated. This conclusion is largely based on the observation that the number of AEC per alveolus is higher than the number of AM or neutrophils at early stages of infections, while phagocytosis rates and cytokine release are comparable or even higher than observed with AM (see Fig 6).

The functions and roles of macrophages during invasive aspergillosis were the focus of experimental studies as well as computational models which indicate a key role in fungal clearance and recognition [23, 58]. Our results suggest that AM are mainly involved in early recognition of swollen conidia and contribute less to fungal clearance than neutrophils and AEC.

We observe a slightly higher importance of AM in low dose scenarios that indicates the importance of dosage in animal models of invasive aspergillosis to ensure transferability of results. However, our results are in line with the observation that in murine infection models neutrophil depletion, but not AM depletion, increases mortality rates [28]. A possible explanation for the underestimated role of AM in our model is that it is based on ordinary differential equations. Therefore, it is not designed to resolve spatial and stochastic phenomena, while agent-based models are suitable to reflect such effects and were applied previously for the confrontation of AM and conidia in the lung [20, 21, 23, 59]. For example, clumping of conidia (*cf.* Fig 4A) in or outside the alveoli may influence the innate immune response.

Since our model focuses on the innate immune response and builds on a simplification of complex interactions during fungal infection, additional functions of AM are potentially not represented in the model. Such functions of AM involve *e.g.* the balance of pro- and anti-inflammatory signaling as well as the support of tissue repair [60, 61]. Further, AM link innate immunity to the adaptive immune system and are important versatile cells to maximize the robustness of the immune system [62, 63]. Further, due to the simplification of signaling, recruitment and orchestration of immune response in our model, specific roles in these cascades of AM as well as other cell types like monocytes and dendritic cells [64] are not covered.

Additional *in silico* and *in vivo* studies are needed to fully understand the roles of AM as well as lung AEC during invasive aspergillosis. Such models and the model presented here are very valuable to develop new treatment approaches and to determine optimal treatment regimens by a combination of approaches. Dynamic optimization has been previously applied to calculate an optimal time-course of treatment protocols for combating infections. This was based on the determination of an optimal usage of antimicrobials and therapies boosting the immune response [65]. For such purposes, our model provides an excellent starting point to identify time-optimal treatment strategies of invasive aspergillosis.

Materials and methods

Model formulation

To formulate a precise but simplistic kinetic model of the innate immune response during invasive aspergillosis, we choose constant, linear or bilinear rate laws depending on the number of influencing entities. This principle ensures a broad functionality of the model while keeping the number of parameters and complexity as low as possible.

We consider three different states, *i.e.*, resting ($\dot{R}$) and swollen conidia ($\dot{S}$) as well as hyphae ($\dot{H}$). Resting conidia are administered to the host's lung at varying quantity R_0. After 3–4h conidia swell in lung alveoli and can be recognized and phagocytosed by host cells [66]. To correctly include the time needed for swelling of conidia, we model the swelling rate as a normal distribution with the mean at time point $r_1 = 4h$ and variance 1h:

$$\dot{R} = \underbrace{-R_0 \, f_n\left(t \mid r_1, 1h\right)}_{\text{swelling}}, \quad f_n(t \mid \mu, \sigma^2) = \frac{1}{\sqrt{2\pi\sigma^2}} e^{-\frac{(t-\mu)^2}{2\sigma^2}}. \tag{1}$$

The time delay of the swelling process cannot be fully resolved by simple linear kinetics which are typically used for growth rates. Further, individual spores do not swell or germinate at the same time delay, as can be seen from germination experiments in our study (see Fig 4B) and others [53]. Hence, we assume as an approximation that the time delay of swelling and germination of spores follows a normal distribution.

Subsequent to swelling, conidia germinate after an additional delay of $s_1 = 3h$ to hyphae [66, 67]. The phagocytosis by immune as well as AEC is modeled by simple bilinear terms with the

specific rates (s_{2-4}):

$$\dot{S} = \underbrace{R_0\, f_n\,(t\,|\,r_1, 1h)}_{\text{swelling}} \underbrace{-S f_n(t\,|\,r_1 + s_1, 1h)}_{\text{germination}} \underbrace{-S(s_2\,M + s_3\,N + s_4\,L)}_{\text{phagocytosis}}. \tag{2}$$

In the multicellular growth state of hyphae the number of *A. fumigatus* cells depends on the rate of germination as well as the growth rate (h_1) of hyphae, which we link to the presence of AEC as a resource for growth. We model killing of hyphae by neutrophils and obtain the following description of hyphal dynamics:

$$\dot{H} = \underbrace{S f_n(t\,|\,r_1 + s_1, 1h)}_{\text{germination}} + \underbrace{h_1 \frac{L}{L_0} H}_{\text{growth}} \underbrace{- h_2\, H\, N}_{\text{killing}}. \tag{3}$$

In our model the number of AEC ($\dot{L}$) is influenced by the lysis induced by fungal hyphae and the damage originating from active AM and neutrophils. The tissue damage by immune cells is often ignored in computational models, but is crucial to understand recruitment and, in particular, depletion of immune cells [68]. To this end, we further connect tissue damage with the pro-inflammatory cytokine level C:

$$\dot{L} = \underbrace{-l_1\, L\, H}_{\text{dissemination}} \underbrace{- L\, C(l_2 N + l_3 M)}_{\text{tissue damage}}. \tag{4}$$

AM are of relevance for recognition and phagocytosis of swollen conidia. In addition to tissue-resident cells, more AM are recruited by transmigration and differentiation of monocytes which circulate in the blood. We assume that this recruitment has a maximal rate of m_1 cells per hour and depends on the pro-inflammatory cytokine level C and macrophage recruitment is further optimized *via* the control variable $u_1(t)$. This time dependent control variable is optimized by dynamic optimization and can vary between 0 (no macrophage recruitment) to 1 (maximal recruitment) at each time point. In a similar way active depletion or deactivation of AM is modeled ($u_2(t)$). Lastly, the number of AM ($\dot{M}$) also depends on the lysis initiated by germinating conidia and therefore we model macrophage dynamics as:

$$\dot{M} = \underbrace{m_1\, C\, u_1}_{\text{recruitment}} \underbrace{- m_2\,(C)\, u_2}_{\text{depletion}} \underbrace{- m_3\, M(S f_n(t\,|\,r_1 + s_1, 1h))}_{\text{lysis by germinating conidia}}. \tag{5}$$

An important role of AM is the release of pro-inflammatory cytokines in response to fungal cells. However, AEC in addition release cytokines and mediate neutrophil recruitment. Thus, we model the dynamics of a pro-inflammatory cytokine level ($\dot{C}$) ranging from 0 (no inflammation) to 1 (maximum inflammation) as follows:

$$\dot{C} = \underbrace{c_1\,(S + H)\, M\,(1 - C)}_{\text{inflammation by AMs}} + \underbrace{c_2\, H\, L\,(1 - C)}_{\text{inflammation by AECs}} \underbrace{- c_3\, C}_{\text{decay}}. \tag{6}$$

It is important to note that based on experimental observations, AEC start releasing cytokines only after conidia had germinated [30] and AM already in response to swollen conidia [7].

Although neutrophils also reside in lung tissue, they are recruited in large quantities from the blood in response to a fungal infection by pro-inflammatory cytokines like interleukin 8

[30]. The kinetics of a neutrophil population($\dot{N}$) is described by:

$$\dot{N} = \underbrace{n_1 \, C \, u_3}_{\text{recruitment}} \underbrace{- n_2 \, (C) \, u_4}_{\text{depletion}} \underbrace{- n_3 \, N \, (S + H)}_{\text{lysis by fungi}} \tag{7}$$

The kinetic parameters are cumbersome to be determined due to the inclusion of optimal control variables and experimental inaccessibility of *in vivo* infection parameters. Nevertheless, we carefully and extensively reviewed published experiments to estimate each parameter (see S1 Appendix). Parameters and cell numbers are determined per murine alveolus.

The above described ODE system and parameters are available as SBML file in S1 File and are stored in the database BioModels [69] under the accession MODEL2105110001.

Constraints and objective of optimization problem.   To determine the optimal innate immune response during invasive aspergillosis, the above described dynamic system has to fulfill the following constraints and objectives. Intuitively, state variables describing cell numbers are positive, pro-inflammatory cytokine level as well as control variables describing recruitment and depletion of immune cells range between 0 and 1:

$$0 \leq \begin{pmatrix} L(t) \\ R(t) \\ S(t) \\ H(t) \\ M(t) \\ N(t) \end{pmatrix} \begin{array}{l} \text{alveolar epithelial cells} \\ \text{resting conidia} \\ \text{swollen conidia} \\ \text{hyphae} \\ \text{alveolar macrophages} \\ \text{neutrophils} \end{array} , \quad \underbrace{0 \leq C(t) \leq 1}_{\text{cytokines}}, \quad \underbrace{0 \leq u_{1-4}(t) \leq 1}_{\text{transmigration}} \tag{8}$$

Host evolution led to the development of immunity which optimizes a trade-off between costs and benefits. Intuitively, minimization of pathogen load is crucial for the host to survive and tissue damage as well as immune functions are costly. By this reasoning we defined two main goals of the host organism. Firstly, active fungal cells (swollen conidia and hyphae) should be minimized at all time points to reduce the risk of systemic infection. Secondly, unnecessary tissue damage *e.g.* by hyperinflammation and collateral damage mediated by immune cells must be avoided. We formalize as objective function:

$$F = \min_{u_{1-4}} \int_0^{T_{max}} \left(o_2 \cdot \frac{S(t)}{r_0} + o_3 \cdot \frac{H(t)}{r_0} - o_1 \cdot \frac{L(t)}{l_0} \right) dt. \tag{9}$$

Here, the calculation as a time integral ensures an optimization over time, rather than an unrealistic end-point minimization. The normalization to the initial cell numbers and equal weighting $o_{1-3} = 0.5$ ensures a balanced and biological meaningful optimization result. As shown in S2 Appendix, considering only one of the objectives leads to undesired dynamics like continued hyphal growth or extensive tissue damage. While the difference between the weightings o_{1-3} influences optimal control dynamics, the magnitude does not change the optimal control qualitatively. Hence, the value $o_{1-3} = 0.5$ is chosen as scaling factor for technical reasons so that numerical issues during optimization are avoided.

Solving the optimization problem and parameter sensitivity

The resulting dynamic optimization problem with continuous state and control variables was solved by a quasi-sequential approach established and implemented by Bartl *et al.* [70]. This

gradient-based method has proven its capability in several previous applications to biological systems [24, 71–74] and ensures fast and robust calculation of the optimal control. To avoid local optima, we perform for each parameter set at least 100 randomizations of the initial solution, which is used to start the optimization process.

To determine the sensitivity of parameters, we sampled 500 parameter sets according to a log-normal distribution, where for each parameter the respective mode (maximum of the density function) corresponds to the literature-based parameter value (see S1 Appendix). The latter ensures that parameter sensitivity is determined in the proximity of the reference parameter set and parameter values are always non-negative. The parameter sensitivity is expressed as the contribution to variance [75] and is based on the Spearman correlation $\rho(p)$ between the parameter value p and the objective function value:

$$ctv_p = \frac{\rho(p)^2}{\sum\limits_p \rho(p)^2}. \tag{10}$$

Our model enables the exploration of different scenarios like different conidia doses and immunodeficiencies. For mice we use as initial conidia burden a dose of 1 conidium per alveolus as 'sublethal' and in low dose scenarios 0.1 which are comparable to *in vivo* experiments. A lack of immune cells like neutropenia or monocytopenia (lack of AM) is simulated by a reduced (1%) initial cell number and rate of recruitment. In a similar way, cytokine release inhibition is simulated by reducing the rates to 1% of the reference value.

Experimental evaluation of fungal and host infection parameters

Fungal strains and cultivation.   *Aspergillus fumigatus* CEA10, *Aspergillus nidulans* FGSC A4, *Aspergillus niger* ATCC 1015 and *Aspergillus terreus* SBUG 844 were grown on *Aspergillus* minimal medium (AMM; containing $70mM\ NaNO_3$, $11.2mM\ KH_2PO_4$, $7mM\ KCl$, $2mM\ MgSO_4$, and $1^{\mu L}/_{mL}$ trace element solution at pH 6.5) and agar plates with 1% (w/v) glucose for 5 days at $37°C$. The trace element solution was composed of $1g\ FeSO_4 \cdot 7H_2O$, $8.8g$ $ZnSO_4 \cdot 7H_2O$, $0.4g\ CuSO_4 \cdot 5H_2O$, $0.15g\ MnSO_4 \cdot H_2O$, $0.1g\ NaB_4O_7 \cdot 10H_2O$, $0.05g\ (NH_4)_6$ $Mo_7O_{24} \cdot 4H_2O$, and ultra-filtrated water to $1000mL$ [76]. All conidia were harvested in sterile, autoclaved water, then filtered through $30\mu m$ filters (MACS Milteny Biotec) and counted with a Thoma chamber.

Germination assay.   Germination assay was performed by inoculating $1 \cdot 10^6$ conidia per mL in RPMI without phenol red (Thermo Fisher Scientific). At different time points pictures were taken using a Keyence BZ-X800 microscope and the number of germinated spores was determined by counting the ratio of spores undergoing germination (germ-tube formation) per field (100 cells).

Cytotoxicity assay.   Human lung AEC A549 (ATCC-CCL 185) were maintained in F12K nutrient medium (Thermo Fisher Scientific) with the addition of 10% (v/v) fetal bovine serum (FBS) (HyClone, GE Life science) at $37°C$ with 5% (v/v) CO_2. Cells of the mouse lung epithelial cell line T7 (ECACC 07021402) were maintained in F12K nutrient medium (Thermo Fisher Scientific) with the addition of 0.5% (v/v) FBS (HyClone, GE Life science) and 0.02% (v/v) Insulin-Transferin-Sodium Selenite (Sigma Aldrich). $2 \cdot 10^5$ cells per well were seeded in 24 well plate $18h$ prior to the experiment. Before infection cells were washed once with sterile phosphate buffered saline (PBS) 1X (Gibco, Thermo Fisher Scientific) and then incubated with conidia based on the different MOIs in DMEM without phenol red (Gibco, Thermo Fisher Scientific) with the addition of 10% (v/v) FBS. Cells and conidia were incubated for $20h$ at $37°C$ with 5% (v/v) CO_2. LDH release was measured using the CyQuant LDH cytotoxicity

assay (Thermo Fisher Scientific) using the manufacturer instructions. The absorbance was determined using a Tecan Infinite 200 (LabX).

Isolation of alveolar epithelial type II cells and AM from mice. A total of eighteen male and female 12–18 weeks old C57BL/6J (The Jackson Laboratory) mice were used. Mice were cared for in accordance with the principles outlined by the European Convention for the Protection of Vertebrate Animals Used for Experimental and Other Scientific Purposes (European Treaty Series, no.123). All animal experiments were in compliance with the German animal protection law and were approved by the responsible federal state authority "Thüringer Landesamt für Lebensmittelsicherheit und Verbraucherschutz" and ethics committee "Beratende Kommission nach §15 Abs. 1 Tierschutzgesetz" (permit no. 03–027/16).

Mice were sacrificed using $125\mu L$ ketamine/xylazine per 20g and the lungs were obtained as previously described [77]. After isolation, the lungs lobes were digested for $45min$ at room temperature in $1mL$ of dispase (Corning) and then the lung parenchyma was separated with the help of tweezers in $7mL$ of DMEM/F12K (Thermo Fisher Scientific) containing $0.01mg$ of DNase (Sigma Aldrich). The cell suspension was first filtered twice: through a $70\mu m$ and then through a $30\mu m$ (MACS, Miltenyi Biotec) filter and finally centrifuged. The pellet was lysed using a red blood cell (RBC) lysis buffer and re-centrifuged.

For their separation cells underwent a double magnetic labeling selection. At first, they were negatively labeled using CD45 (macrophages), CD16/32 (B/NK cells), anti-Ter (erythrocytes), CD31 (endothelial cells) (Miltyenyi Biotec) and anti-t1α (alveolar epithelial type I cells) (Novus Biologicals), biotin-linked antibodies. Secondly the negative fraction was collected and positively selected for alveolar epithelial type II cells using a CD326/EpCAM antibody (eBioscience). Both labeling steps were perfomed at $4˚C$ for $30min$, and followed by a second labeling with Anti-Biotin Microbeads Ultrapure (Miltenyi Biotec) for $15min$ at $4˚C$. The separation was performed using an autoMACS Pro Separator machine (Miltyenyi Biotec). The final cell suspension containing type II AEC was resuspended in mouse tracheal epithelial cells (MTEC) basic medium [78]: DMEM-F12K +1% HEPES, Na-bicarbonate, L-glutamine, penicillin-streptomycin, 0.1% amphotericin B (Gibco) supplemented with 0.001% Insulin-transferrin (Gibco), $0.1^{ug}/_{mL}$ cholera toxin (Sigma Aldrich), $25^{ng}/_{mL}$ epidermal growth factor (Invitrogen) and mice fibroblast growth factor 7 (R&D system), $30^{ug}/_{mL}$ bovine pituitary extract (Gibco), $30^{ng}/_{mL}$ multilinear hemopoietic growth factor, $50^{ng}/_{mL}$ human fibroblastic growth factor 10 (R&D system), 5% FBS, $0.01\mu M$ retinoic acid (Sigma Aldrich) and $10\mu M$ Rho kinase inhibitor (ROCK) (Thermo Fisher Scientific).

The isolation of AM was performed similarly, only using the first labeling step with CD45 antibodies. AM were re-suspended in MTEC basic medium with the addition of 10% (v/v) FBS.

Due to the necessity of using all the cells for experiment, the purity of the isolated cells was not assessed after every experiment, but as previously demonstrated this protocol assures a purity between 98—99% [77]. The percentage of viable cells was measured using Trypan blue and it was between 75—90% depending on the mice. From each mouse, a total of $1 \cdot 10^6$ cells were seeded onto 8 well Millicells slides (Merc, Millipore), pre-coated with $100^{ug}/_{mL}$ of fibronectin (Sigma Aldrich), for AEC, and incubated at $37˚C$ and 5% (v/v) CO_2. The medium was changed every 2 days and the cells were left to rest for 7 days prior the experiment.

Infection with *A. fumigatus* and cytokine measurement. Alveolar epithelial type II cells were infected with *A. fumigatus* CEA10 conidia at a multiplicity of infection (MOI) of 5, for 4, 6, 10, and 24h. At these time points the supernatant was collected, centrifuged at $300 \cdot g$ for 5 min and then stored at -20˚C for 24h until measurements. The levels of interleukin (IL)-6 and tumor necrosis factor (TNF)-α were detected using ELISA kits (Biolegend) following the manufacturer's instructions.

Supporting information

S1 Appendix. Parameter estimation. Documentation of parameter estimation and calculation.
(PDF)

S2 Appendix. Objective function weighting. Influence of weighting innate immune response objectives.
(PDF)

S1 File. SBML model description. The described model of invasive aspergillosis is provided as SBML and COPASI file. To enable simulation, control variables u_{1-4} are fixed. Further, the model is archived in EBI BioModels under the accession MODEL2105110001.
(XML)

S1 Fig. Influence of MOI on cytotoxicity of *Aspergillus spp*. against epithelial cells. In addition to the depicted LDH release measurements of epithelial cells upon 24h co-incubation with *Aspergillus spp.* at an *MOI* = 5 (main text Fig 4D and 4E), cytotoxicity was measured for *MOI* = 2 and *MOI* = 10 for human A549 cells to demonstrate the influence of fungal burden.
(TIF)

Acknowledgments

Author Contributions

Conceptualization: Jan Ewald, Axel A. Brakhage, Christoph Kaleta.

Data curation: Jan Ewald, Flora Rivieccio.

Formal analysis: Jan Ewald.

Funding acquisition: Stefan Schuster, Axel A. Brakhage.

Investigation: Jan Ewald, Flora Rivieccio.

Methodology: Jan Ewald, Flora Rivieccio, Lukáš Radosa.

Resources: Stefan Schuster, Axel A. Brakhage.

Software: Jan Ewald.

Supervision: Stefan Schuster, Axel A. Brakhage, Christoph Kaleta.

Validation: Flora Rivieccio, Lukáš Radosa.

Visualization: Jan Ewald.

Writing – original draft: Jan Ewald, Christoph Kaleta.

Writing – review & editing: Flora Rivieccio, Lukáš Radosa, Stefan Schuster, Axel A. Brakhage, Christoph Kaleta.

References

1. Mizgerd JP. Lung infection—a public health priority. PLoS Medicine. 2006; 3(2):e76. https://doi.org/10.1371/journal.pmed.0030076 PMID: 16401173

2. Vento S, Cainelli F, Temesgen Z. Lung infections after cancer chemotherapy. The Lancet Oncology. 2008; 9(10):982–992. https://doi.org/10.1016/S1470-2045(08)70255-9 PMID: 19071255

3. Brakhage AA, Langfelder K. Menacing mold: the molecular biology of *Aspergillus fumigatus*. Annual Reviews in Microbiology. 2002; 56(1):433–455. https://doi.org/10.1146/annurev.micro.56.012302.160625 PMID: 12142473

4. Tekaia F, Latgé JP. *Aspergillus fumigatus*: saprophyte or pathogen? Current Opinion in Microbiology. 2005; 8(4):385–392. https://doi.org/10.1016/j.mib.2005.06.017 PMID: 16019255

5. Dagenais TR, Keller NP. Pathogenesis of *Aspergillus fumigatus* in invasive aspergillosis. Clinical Microbiology Reviews. 2009; 22(3):447–465. https://doi.org/10.1128/CMR.00055-08 PMID: 19597008

6. Scharf DH, Heinekamp T, Remme N, Hortschansky P, Brakhage AA, Hertweck C. Biosynthesis and function of gliotoxin in *Aspergillus fumigatus*. Applied Microbiology and Biotechnology. 2012; 93 (2):467–472. https://doi.org/10.1007/s00253-011-3689-1 PMID: 22094977

7. Latgé JP, Chamilos G. *Aspergillus fumigatus* and Aspergillosis in 2019. Clinical Microbiology Reviews. 2019; 33(1). https://doi.org/10.1128/cmr.00140-18 PMID: 31722890

8. Osherov N. Interaction of the pathogenic mold *Aspergillus fumigatus* with lung epithelial cells. Frontiers in Microbiology. 2012; 3:346. https://doi.org/10.3389/fmicb.2012.00346 PMID: 23055997

9. Balloy V, Chignard M. The innate immune response to *Aspergillus fumigatus*. Microbes and Infection. 2009; 11(12):919–927. https://doi.org/10.1016/j.micinf.2009.07.002 PMID: 19615460

10. Brown SP, Cornforth DM, Mideo N. Evolution of virulence in opportunistic pathogens: generalism, plasticity, and control. Trends in Microbiology. 2012; 20(7):336–342. https://doi.org/10.1016/j.tim.2012.04.005 PMID: 22564248

11. Dragonetti G, Criscuolo M, Fianchi L, Pagano L. Invasive Aspergillosis in Acute Myeloid Leukemia: Are We Making Progress in Reducing Mortality? Medical Mycology. 2017; 55(1):82–86. https://doi.org/10.1093/mmy/myw114 PMID: 27915304

12. Taccone FS, Van den Abeele AM, Bulpa P, Misset B, Meersseman W, Cardoso T, et al. Epidemiology of invasive aspergillosis in critically ill patients: clinical presentation, underlying conditions, and outcomes. Critical Care. 2015; 19(1):7. https://doi.org/10.1186/s13054-014-0722-7 PMID: 25928694

13. Bartoletti M, Pascale R, Cricca M, Rinaldi M, Maccaro A, Bussini L, et al. Epidemiology of invasive pulmonary aspergillosis among COVID-19 intubated patients: a prospective study. Clinical Infectious Diseases. 2020. https://doi.org/10.1093/cid/ciaa1065 PMID: 32719848

14. Weir HK, Thompson TD, Soman A, Møller B, Leadbetter S. The past, present, and future of cancer incidence in the United States: 1975 through 2020. Cancer. 2015; 121(11):1827–1837. https://doi.org/10.1002/cncr.29258 PMID: 25649671

15. Mistry M, Parkin D, Ahmad AS, Sasieni P. Cancer incidence in the United Kingdom: projections to the year 2030. British Journal of Cancer. 2011; 105(11):1795. https://doi.org/10.1038/bjc.2011.430 PMID: 22033277

16. Wynn JJ, Alexander CE. Increasing organ donation and transplantation: the US experience over the past decade. Transplant International. 2011; 24(4):324–332. https://doi.org/10.1111/j.1432-2277.2010.01201.x PMID: 21208297

17. Granich R, Gupta S, Hersh B, Williams B, Montaner J, Young B, et al. Trends in AIDS deaths, new infections and ART coverage in the top 30 countries with the highest AIDS mortality burden; 1990–2013. PloS One. 2015; 10(7):e0131353. https://doi.org/10.1371/journal.pone.0131353 PMID: 26147987

18. Hoenigl M. Invasive fungal disease complicating coronavirus disease 2019: when it rains, it spores. Clinical Infectious Diseases. 2020. https://doi.org/10.1093/cid/ciaa1342 PMID: 32887998

19. Tanaka RJ, Boon NJ, Vrcelj K, Nguyen A, Vinci C, Armstrong-James D, et al. *In silico* modeling of spore inhalation reveals fungal persistence following low dose exposure. Scientific Reports. 2015; 5:13958. https://doi.org/10.1038/srep13958 PMID: 26364644

20. Pollmächer J, Figge MT. Deciphering chemokine properties by a hybrid agent-based model of *Aspergillus fumigatus* infection in human alveoli. Frontiers in Microbiology. 2015; 6:503. https://doi.org/10.3389/fmicb.2015.00503 PMID: 26074897

21. Oremland M, Michels KR, Bettina AM, Lawrence C, Mehrad B, Laubenbacher R. A computational model of invasive aspergillosis in the lung and the role of iron. BMC Systems Biology. 2016; 10(1):34. https://doi.org/10.1186/s12918-016-0275-2 PMID: 27098278

22. Pollmächer J, Timme S, Schuster S, Brakhage AA, Zipfel PF, Figge MT. Deciphering the counterplay of *Aspergillus fumigatus* infection and host inflammation by evolutionary games on graphs. Scientific Reports. 2016; 6:27807. https://doi.org/10.1038/srep27807 PMID: 27291424

23. Blickensdorf M, Timme S, Figge MT. Comparative Assessment of Aspergillosis by Virtual Infection Modeling in Murine and Human Lung. Frontiers in Immunology. 2019; 10. https://doi.org/10.3389/fimmu.2019.00142 PMID: 30804941

24. Ewald J, Sieber P, Garde R, Lang SN, Schuster S, Ibrahim B. Trends in mathematical modeling of host–pathogen interactions. Cellular and Molecular Life Sciences. 2019; p. 1–14. https://doi.org/10.1007/s00018-019-03382-0 PMID: 31776589

25. Blickensdorf M, Timme S, Figge MT. Hybrid agent-based modeling of *Aspergillus fumigatus* infection to quantitatively investigate the role of pores of Kohn in human alveoli. Frontiers in Microbiology. 2020; 11:1951. https://doi.org/10.3389/fmicb.2020.01951 PMID: 32903715

26. Philippe B, Ibrahim-Granet O, Prevost M, Gougerot-Pocidalo M, Perez MS, Van der Meeren A, et al. Killing of *Aspergillus fumigatus* by alveolar macrophages is mediated by reactive oxidant intermediates. Infection and Immunity. 2003; 71(6):3034–3042. https://doi.org/10.1128/IAI.71.6.3034-3042.2003 PMID: 12761080

27. Taramelli D, Malabarba M, Sala G, Basilico N, Cocuzza G. Production of cytokines by alveolar and peritoneal macrophages stimulated by *Aspergillus fumigatus* conidia or hyphae. Journal of Medical and Veterinary Mycology. 1996; 34(1):49–56. https://doi.org/10.1080/02681219680000081 PMID: 8786471

28. Mircescu MM, Lipuma L, van Rooijen N, Pamer EG, Hohl TM. Essential role for neutrophils but not alveolar macrophages at early time points following *Aspergillus fumigatus* infection. The Journal of Infectious Diseases. 2009; 200(4):647–656. https://doi.org/10.1086/600380 PMID: 19591573

29. Wasylnka JA, Moore MM. *Aspergillus fumigatus* conidia survive and germinate in acidic organelles of A549 epithelial cells. Journal of Cell Science. 2003; 116(8):1579–1587. https://doi.org/10.1242/jcs.00329 PMID: 12640041

30. Balloy V, Sallenave JM, Wu Y, Touqui L, Latgé JP, Si-Tahar M, et al. *Aspergillus fumigatus*-induced interleukin-8 synthesis by respiratory epithelial cells is controlled by the phosphatidylinositol 3-kinase, p38 MAPK, and ERK1/2 pathways and not by the toll-like receptor-MyD88 pathway. Journal of Biological Chemistry. 2008; 283(45):30513–30521. https://doi.org/10.1074/jbc.M803149200

31. Jhingran A, Kasahara S, Shepardson KM, Junecko BAF, Heung LJ, Kumasaka DK, et al. Compartment-specific and sequential role of MyD88 and CARD9 in chemokine induction and innate defense during respiratory fungal infection. PLoS Pathogens. 2015; 11(1):e1004589. https://doi.org/10.1371/journal.ppat.1004589 PMID: 25621893

32. Shudo E, Iwasa Y. Dynamic optimization of host defense, immune memory, and post-infection pathogen levels in mammals. Journal of Theoretical Biology. 2004; 228(1):17–29. https://doi.org/10.1016/j.jtbi.2003.12.001 PMID: 15064080

33. Lenhart S, Workman JT. Optimal control applied to biological models. CRC press; 2007.

34. Dühring S, Ewald J, Germerodt S, Kaleta C, Dandekar T, Schuster S. Modelling the host–pathogen interactions of macrophages and *Candida albicans* using Game Theory and dynamic optimization. Journal of The Royal Society Interface. 2017; 14(132):20170095. https://doi.org/10.1098/rsif.2017.0095 PMID: 28701506

35. McDade TW, Georgiev AV, Kuzawa CW. Trade-offs between acquired and innate immune defenses in humans. Evolution, Medicine, and Public Health. 2016; 2016(1):1–16. https://doi.org/10.1093/emph/eov033 PMID: 26739325

36. Desoubeaux G, Cray C. Rodent models of invasive aspergillosis due to *Aspergillus fumigatus*: still a long path toward standardization. Frontiers in Microbiology. 2017; 8:841. https://doi.org/10.3389/fmicb.2017.00841 PMID: 28559881

37. Desoubeaux G, Cray C. Animal models of aspergillosis. Comparative Medicine. 2018; 68(2):109–123. PMID: 29663936

38. Heinekamp T, Schmidt H, Lapp K, Pähtz V, Shopova I, Köster-Eiserfunke N, et al. Interference of *Aspergillus fumigatus* with the immune response. In: Seminars in Immunopathology. vol. 37. Springer; 2015. p. 141–152.

39. Knox BP, Huttenlocher A, Keller NP. Real-time visualization of immune cell clearance of *Aspergillus fumigatus* spores and hyphae. Fungal Genetics and Biology. 2017; 105:52–54. https://doi.org/10.1016/j.fgb.2017.05.005 PMID: 28559109

40. Tsiantis N, Balsa-Canto E, Banga JR. Optimality and identification of dynamic models in systems biology: an inverse optimal control framework. Bioinformatics. 2018; 34(14):2433–2440. https://doi.org/10.1093/bioinformatics/bty139 PMID: 29522196

41. Stone KC, Mercer RR, Gehr P, Stockstill B, Crapo JD, et al. Allometric relationships of cell numbers and size in the mammalian lung. American Journal of Respiratory Cell and Molecular Biology. 1992; 6 (2):235–43. https://doi.org/10.1165/ajrcmb/6.2.235 PMID: 1540387

42. Knust J, Ochs M, Gundersen HJG, Nyengaard JR. Stereological estimates of alveolar number and size and capillary length and surface area in mice lungs. The Anatomical Record: Advances in Integrative Anatomy and Evolutionary Biology: Advances in Integrative Anatomy and Evolutionary Biology. 2009; 292(1):113–122. https://doi.org/10.1002/ar.20747 PMID: 19115381

43. Guillot L, Nathan N, Tabary O, Thouvenin G, Le Rouzic P, Corvol H, et al. Alveolar epithelial cells: master regulators of lung homeostasis. The International Journal of Biochemistry & Cell Biology. 2013; 45 (11):2568–2573. https://doi.org/10.1016/j.biocel.2013.08.009 PMID: 23988571

44. Wong MH, Johnson MD. Differential response of primary alveolar type I and type II cells to LPS stimulation. PLoS One. 2013; 8(1):e55545. https://doi.org/10.1371/journal.pone.0055545 PMID: 23383221

45. Amich J, Mokhtari Z, Strobel M, Vialetto E, Sheta D, Yu Y, et al. Three-dimensional light sheet fluorescence microscopy of lungs to dissect local host immune-*Aspergillus fumigatus* interactions. mBio. 2020; 11(1). https://doi.org/10.1128/mBio.02752-19 PMID: 32019790

46. Kalleda N, Amich J, Arslan B, Poreddy S, Mattenheimer K, Mokhtari Z, et al. Dynamic immune cell recruitment after murine pulmonary *Aspergillus fumigatus* infection under different immunosuppressive regimens. Frontiers in Microbiology. 2016; 7:1107. https://doi.org/10.3389/fmicb.2016.01107 PMID: 27468286

47. Sheppard DC, Rieg G, Chiang LY, Filler SG, Edwards JE, Ibrahim AS. Novel inhalational murine model of invasive pulmonary aspergillosis. Antimicrobial Agents and Chemotherapy. 2004; 48(5):1908–1911. https://doi.org/10.1128/AAC.48.5.1908-1911.2004 PMID: 15105158

48. Duong M, Ouellet N, Simard M, Bergeron Y, Olivier M, Bergeron MG. Kinetic study of host defense and inflammatory response to *Aspergillus fumigatus* in steroid-induced immunosuppressed mice. The Journal of Infectious Diseases. 1998; 178(5):1472–1482. https://doi.org/10.1086/314425 PMID: 9780270

49. Borger P, Koeter G, Timmerman J, Vellenga E, Tomee J, Kauffman H. Proteases from *Aspevgillus fumigatus* Induce Interleukin (IL)-6 and IL-8 Production in Airway Epithelial Cell Lines by Transcriptional Mechanisms. The Journal of Infectious Diseases. 1999; 180(4):1267–1274. https://doi.org/10.1086/315027 PMID: 10479157

50. Cenci E, Mencacci A, Casagrande A, Mosci P, Bistoni F, Romani L. Impaired antifungal effector activity but not inflammatory cell recruitment in interleukin-6-deficient mice with invasive pulmonary aspergillosis. The Journal of Infectious Diseases. 2001; 184(5):610–617. https://doi.org/10.1086/322793 PMID: 11494166

51. Song HS, Cannon WR, Beliaev AS, Konopka A. Mathematical modeling of microbial community dynamics: a methodological review. Processes. 2014; 2(4):711–752. https://doi.org/10.3390/pr2040711

52. Cannon WR. Simulating metabolism with statistical thermodynamics. PLoS One. 2014; 9(8):e103582. https://doi.org/10.1371/journal.pone.0103582 PMID: 25089525

53. Araujo R, Rodrigues AG. Variability of germinative potential among pathogenic species of *Aspergillus*. Journal of Clinical Microbiology. 2004; 42(9):4335–4337. https://doi.org/10.1128/JCM.42.9.4335-4337.2004 PMID: 15365039

54. Rhodes JC. *Aspergillus fumigatus*: growth and virulence. Medical Mycology. 2006; 44(Supplement_1): S77–S81. https://doi.org/10.1080/13693780600779419 PMID: 17050423

55. Caffrey-Carr AK, Kowalski CH, Beattie SR, Blaseg NA, Upshaw CR, Thammahong A, et al. Interleukin 1α is critical for resistance against highly virulent *Aspergillus fumigatus* isolates. Infection and immunity. 2017; 85(12):e00661–17. https://doi.org/10.1128/IAI.00661-17 PMID: 28947643

56. Paulussen C, Hallsworth JE, Álvarez-Pérez S, Nierman WC, Hamill PG, Blain D, et al. Ecology of aspergillosis: insights into the pathogenic potency of *Aspergillus fumigatus* and some other *Aspergillus* species. Microbial Biotechnology. 2017; 10(2):296–322. https://doi.org/10.1111/1751-7915.12367 PMID: 27273822

57. Bonnett CR, Cornish EJ, Harmsen AG, Burritt JB. Early neutrophil recruitment and aggregation in the murine lung inhibit germination of *Aspergillus fumigatus* conidia. Infection and Immunity. 2006; 74 (12):6528–6539. https://doi.org/10.1128/IAI.00909-06 PMID: 16920786

58. Rosowski EE, Raffa N, Knox BP, Golenberg N, Keller NP, Huttenlocher A. Macrophages inhibit *Aspergillus fumigatus* germination and neutrophil-mediated fungal killing. PLoS Pathogens. 2018; 14(8): e1007229. https://doi.org/10.1371/journal.ppat.1007229 PMID: 30071103

59. Tokarski C, Hummert S, Mech F, Figge MT, Germerodt S, Schroeter A, et al. Agent-based modeling approach of immune defense against spores of opportunistic human pathogenic fungi. Frontiers in Microbiology. 2012; 3:129. https://doi.org/10.3389/fmicb.2012.00129 PMID: 22557995

60. Wynn TA, Vannella KM. Macrophages in tissue repair, regeneration, and fibrosis. Immunity. 2016; 44 (3):450–462. https://doi.org/10.1016/j.immuni.2016.02.015 PMID: 26982353

61. Allard B, Panariti A, Martin JG. Alveolar macrophages in the resolution of inflammation, tissue repair, and tolerance to infection. Frontiers in Immunology. 2018; 9:1777. https://doi.org/10.3389/fimmu.2018.01777 PMID: 30108592

62. Sales-Campos H, Tonani L, Cardoso CRB, Kress MRVZ. The immune interplay between the host and the pathogen in *Aspergillus fumigatus* lung infection. BioMed Research International. 2013; 2013. https://doi.org/10.1155/2013/693023 PMID: 23984400

63. Espinosa V, Rivera A. First line of defense: innate cell-mediated control of pulmonary aspergillosis. Frontiers in Microbiology. 2016; 7:272. https://doi.org/10.3389/fmicb.2016.00272 PMID: 26973640

64. Guo Y, Kasahara S, Jhingran A, Tosini NL, Zhai B, Aufiero MA, et al. During Aspergillus infection, monocyte-derived DCs, neutrophils, and plasmacytoid DCs enhance innate immune defense through CXCR3-dependent crosstalk. Cell Host & Microbe. 2020; 28(1):104–116. https://doi.org/10.1016/j.chom.2020.05.002 PMID: 32485165

65. Stengel RF, Ghigliazza RM, Kulkarni NV. Optimal enhancement of immune response. Bioinformatics. 2002; 18(9):1227–1235. https://doi.org/10.1093/bioinformatics/18.9.1227 PMID: 12217914

66. Dague E, Alsteens D, Latgé JP, Dufrêne YF. High-resolution cell surface dynamics of germinating *Aspergillus fumigatus* conidia. Biophysical Journal. 2008; 94(2):656–660. https://doi.org/10.1529/biophysj.107.116491 PMID: 17890393

67. Kwon-Chung KJ, Sugui JA. *Aspergillus fumigatus*—what makes the species a ubiquitous human fungal pathogen? PLoS Pathogens. 2013; 9(12):e1003743. https://doi.org/10.1371/journal.ppat.1003743 PMID: 24348239

68. Cicchese JM, Evans S, Hult C, Joslyn LR, Wessler T, Millar JA, et al. Dynamic balance of pro-and anti-inflammatory signals controls disease and limits pathology. Immunological Reviews. 2018; 285(1):147–167. https://doi.org/10.1111/imr.12671 PMID: 30129209

69. Malik-Sheriff RS, Glont M, Nguyen TV, Tiwari K, Roberts MG, Xavier A, et al. BioModels—15 years of sharing computational models in life science. Nucleic Acids Research. 2020; 48(D1):D407–D415. https://doi.org/10.1093/nar/gkz1055 PMID: 31701150

70. Bartl M, Li P, Biegler LT. Improvement of state profile accuracy in nonlinear dynamic optimization with the quasi-sequential approach. AIChE Journal. 2011; 57(8):2185–2197. https://doi.org/10.1002/aic.12437

71. Wessely F, Bartl M, Guthke R, Li P, Schuster S, Kaleta C. Optimal regulatory strategies for metabolic pathways in *Escherichia coli* depending on protein costs. Molecular Systems Biology. 2011; 7(1). https://doi.org/10.1038/msb.2011.46 PMID: 21772263

72. Bartl M, Kötzing M, Schuster S, Li P, Kaleta C. Dynamic optimization identifies optimal programmes for pathway regulation in prokaryotes. Nature Communications. 2013; 4:2243. https://doi.org/10.1038/ncomms3243 PMID: 23979724

73. Bartl M, Pfaff M, Ghallab A, Driesch D, Henkel SG, Hengstler JG, et al. Optimality in the zonation of ammonia detoxification in rodent liver. Archives of Toxicology. 2015; 89(11):2069–2078. https://doi.org/10.1007/s00204-015-1596-4 PMID: 26438405

74. Ewald J, Bartl M, Kaleta C. Deciphering the regulation of metabolism with dynamic optimization: an overview of recent advances. Biochemical Society Transactions. 2017; 45(4):1035–1043. https://doi.org/10.1042/BST20170137 PMID: 28754658

75. Groen EA, Bokkers EA, Heijungs R, de Boer IJ. Methods for global sensitivity analysis in life cycle assessment. The International Journal of Life Cycle Assessment. 2017; 22(7):1125–1137. https://doi.org/10.1007/s11367-016-1217-3

76. Brakhage AA, Van den Brulle J. Use of reporter genes to identify recessive trans-acting mutations specifically involved in the regulation of *Aspergillus nidulans* penicillin biosynthesis genes. Journal of Bacteriology. 1995; 177(10):2781–2788. https://doi.org/10.1128/jb.177.10.2781-2788.1995 PMID: 7677843

77. Sinha M, Lowell CA. Isolation of highly pure primary mouse alveolar epithelial type II cells by flow cytometric cell sorting. Bio-protocol. 2016; 6(22). https://doi.org/10.21769/BioProtoc.2013 PMID: 28180137

78. You Y, Richer EJ, Huang T, Brody SL. Growth and differentiation of mouse tracheal epithelial cells: selection of a proliferative population. American Journal of Physiology-Lung Cellular and Molecular Physiology. 2002; 283(6):L1315–L1321. https://doi.org/10.1152/ajplung.00169.2002 PMID: 12388377